JOURNAL OF APPLIED PHYSICS **114**, 064504 (2013)

Trapping behavior of Shockley-Read-Hall recombination centers in silicon solar cells

R. Gogolin[1] and N. P. Harder[1,2,a)]
[1]*Institute for Solar Energy Research Hamelin (ISFH), Am Ohrberg 1, 31860 Emmerthal, Germany*
[2]*Institute of Electronic Materials and Devices, University of Hannover, Schneiderberg 32, 30167 Hannover, Germany*

(Received 11 June 2013; accepted 26 July 2013; published online 9 August 2013)

We investigate the correlation between increased apparent carrier lifetime in photoconductance-based lifetime measurements and actually reduced recombination lifetime as measured by photoluminescence measurements. These findings are further reconfirmed by *I-V* curve measurements of solar cells. In particular, we show experimental results for lifetime samples and solar cells with and without hydrogen passivation. In the samples and solar cells without hydrogen passivation, we find both a stronger trapping behavior and a lower recombination lifetime. Our model provides a consistent description of the observation of both, the increased apparent lifetime from carrier trapping and the decreasing recombination lifetime. In our model, both are caused by a single physical mechanism; i.e., by Recombination-Active-Trap (RAT) states. Upon fitting the experimental lifetime data, we find that the RAT-defect parameters for the hydrogen-passivated and non-hydrogen-passivated lifetime samples and solar cells are identical except for the defect concentration: hydrogen-passivation reduced the defect density by 50% in both, the lifetime samples and solar cells. We conclude that trapping should be considered as an indication for hidden, yet potentially strongly increased, low injection recombination activity. © *2013 AIP Publishing LLC*. [http://dx.doi.org/10.1063/1.4817910]

I. INTRODUCTION

Shockley and Read[1] and Hall[2] described the recombination of charge carriers in semiconductors via electronic states in the bandgap (SRH recombination). The associated recombination rate R_{SRH} and recombination lifetime $\tau_{SRH} = \Delta n/R_{SRH}$ are an important measure of the material quality of silicon, where Δn is the excess charge carrier concentration.

The lifetime is also influenced by radiative recombination[3–5] and Auger recombination.[6–11] However, under the typical low level injection operating conditions of most silicon solar cells, the effective carrier lifetime in silicon wafers is dominated by SRH recombination in the volume of the material and SRH-type recombination via electronic states at the surfaces.[12,13]

The effective charge carrier lifetime in a sample can be determined, for example, via transient or (quasi) steady state photo conductance measurements[14] or infrared lock-in thermography.[15,16] Unfortunately, artefacts often distort the measurements of the effective lifetime in low level injection close to the maximum power point of solar cell operation. Temporary capture of minority charge carriers is known to cause very large apparent charge carrier lifetimes that are far in excess of the recombination lifetime that determines device characteristics such as, for example, the voltage of the solar cell. The description of such trapping effects is traditionally done via the model of Hornbeck and Haynes (H&H)[17–19] and can be regarded as a special case of the mechanism described by Shockley, Read, and Hall, i.e., the H&H model assumes states within the bandgap with electronic transitions only between the trap state and the minority charge carrier band. However, McIntosh, Paudyal, and Macdonald[20] have shown that the temperature dependence of the trapping-effect in the apparent lifetime signal can be much more adequately described by allowing for nonzero, yet, nevertheless, very small, majority carrier capture cross sections. This is essentially equivalent to using the SRH recombination mechanism. In this case, numerical equation solving is required for accounting for the concentration of trapped carriers, which give rise to the trapping effects in photo conductance based lifetime determination, such as in quasi steady state photo conductance measurements.

However, in our previous work,[21] we have shown that trapping effects are often correlated with a reduction of the charge carrier lifetime within the low level injection regime. We extended the approach of using SRH statistics for simultaneous describing both, trapping related enhancement of the apparent lifetime in QSSPC[22] measurements and the decrease of the recombination lifetime in low level injection as observable in photoluminescence (PL) measurements[23–25] by a single physical mechanism; i.e., by Recombination-Active-Trap (RAT) states.

In this work, we further elucidate the correlation between increased apparent carrier lifetime in QSSPC lifetime measurements and actually reduced recombination lifetime. We present a detailed analysis of the influence of the RAT defect parameters on the apparent carrier lifetime and the actual recombination lifetime. We show experimental results for lifetime samples and solar cells to provide experimental proof of our model.

a)Now with Total New Energies USA, Inc. Electronic mail: Nils.Harder@Total.com.

II. RECOMBINATION AND TRAPPING MODEL

McIntosh *et al.*[19] recently presented a procedure to determine the dependence of photoconductance lifetime on the occupation of multiple defects. For this purpose, they used SRH recombination statistics to describe the temperature dependence of trapping.

In our description of trapping related recombination effects, we also use the SRH formalism and trap states with cross section for capturing majority charge carriers larger than zero, but potentially several orders of magnitude smaller than the minority capture cross section. In this way, we define a Recombination-Active Trap state (RAT). This type of defect state is formally a SRH recombination center but additionally causes trapping due to its highly asymmetric capture cross sections $\sigma_{p,RAT}$ and $\sigma_{n,RAT}$.

In the following discussion, we assume p-type material, and therefore $\sigma_{p,RAT} \ll \sigma_{n,RAT}$ in order that RAT-states have a trap-character for electrons. We assume RAT-defect states within the bandgap with the density N_{RAT} and the energy level E_{RAT}. The associated RAT-lifetime is $\tau_{RAT} = \Delta n/R_{RAT}$, where R_{RAT} is the recombination rate as calculated by the SRH formalism. Additionally to these trap states, we assume the presence of other electronic defect states within the bandgap with the density N_{SRH}, the energy level E_{SRH} and the electron and hole capture-cross-sections $\sigma_{n,SRH}$ and $\sigma_{p,SRH}$ resulting in the associated SRH-lifetime $\tau_{SRH} = \Delta n/R_{SRH}$. Figure 1 shows a schematic representation of the electronic states within a semiconductor, alongside with the electronic transitions that are considered in our model. The resulting (cumulative) recombination lifetime is $\tau_r = \Delta n/(R_{SRH} + R_{RAT}) = \Delta n/R$.

In accordance to the H&H model, we have to consider that minority charge carriers are temporary captured in RAT-states. Therefore, the assumption $\Delta n = \Delta p$, i.e., the same density of excess charge carriers in valence and conduction band does not apply since there is a lower minority excess carrier density Δn in the conduction band than majority excess carrier density Δp in the valence band, i.e., $\Delta n < \Delta p$. The application of the non-valid assumption $\Delta n = \Delta p$ consequently leads to an overestimation of the excess minority carrier concentration and thus as an increased apparent lifetime $\tau_{app} = \Delta n_{app}/R$.

That is, just as is known from trap states in the H&H model, RAT-states obscure the recombination lifetime by an increased apparent lifetime. However, different to the H&H model, the RAT defect states considered here do have non-zero capture cross sections for the majority charge carriers. Therefore, RAT states do not only cause trapping but additionally cause a reduction of the recombination lifetime. It is important to understand that this effect is not the result of an unrealistic or exotic configuration. Instead, the assumption of a vanishing cross section for the pure trap states in the H&H model is a highly idealized assumption, and it is plausible that trap states within the band gap also interact with the majority carriers, i.e., that they have a non-vanishing recombination activity and are recombination active trap (RAT) states.

Figure 2 shows an example of lifetime calculations, where the SRH-lifetime τ_{SRH} (dotted line) is the carrier lifetime as given by the regular SRH defects (see Table I), where the majority carrier capture cross section is not vastly smaller than that of the minorities. Correspondingly, Figure 2 shows also the RAT-lifetime τ_{RAT} (double dotted line) according to the RAT states. These two lifetimes τ_{SRH} and τ_{RAT} would be present separately, if only the SRH defects or the RAT defects were present. For the simultaneous presence of both types of defects, Figure 2 also plots the total recombination lifetime τ_r and the apparent lifetime τ_{app} for the defect parameters given in Table I assuming a doping concentration of $N_A = 10^{15}\,\mathrm{cm}^{-3}$.

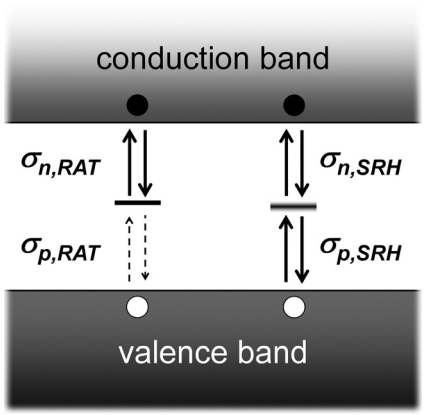

FIG. 1. Schematic representation of the electronic states within a semiconductor, alongside with the electronic transitions that are considered in our model.

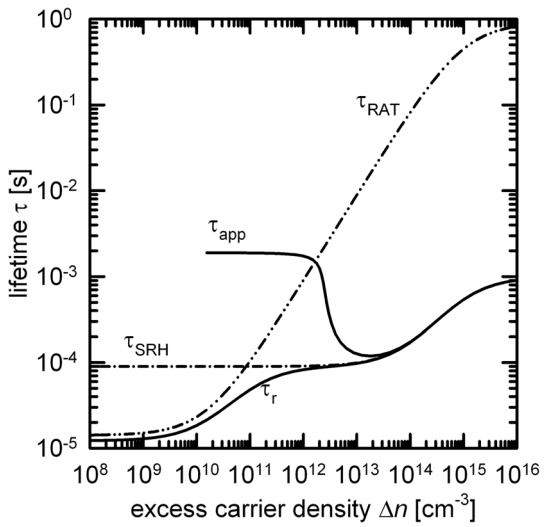

FIG. 2. SRH-lifetime τ_{SRH}, RAT-lifetime τ_{RAT}, total recombination lifetime τ_r and apparent lifetime τ_{app} shown for the defect parameters given in Table I and for a doping concentration of $N_A = 10^{15}\,\mathrm{cm}^{-3}$.

TABLE I. Defect parameters related to Figure 2.

Parameter	SRH-state	RAT-state
E_t - E_V (eV)	0.55	0.55
N_t (cm^{-3})	1×10^{12}	1×10^{13}
σ_n (cm^2)	1×10^{-15}	1×10^{-16}
σ_p (cm^2)	1×10^{-15}	1×10^{-20}

A. Variation of the majority capture cross section $\sigma_{p,RAT}$ of the RAT-state

The ratio between the majority capture cross section $\sigma_{p,RAT}$ and the minority capture cross section $\sigma_{n,RAT}$ defines whether the RAT-defect tends more to behave like a traditional H&H trap or more like a typical SRH recombination center. If the majority capture cross section of the RAT-defects is equal to zero, i.e., $\sigma_{p,RAT} = 0$, the recombination lifetime is only affected by the SRH-defect. This special case complies with the H&H model. If $\sigma_{p,RAT}$ becomes non-zero and increases, the recombination via the RAT-defect increases and the (cumulative) recombination lifetime τ_r decreases. At the same time, the electron concentration trapped within the RAT-defects decreases and consequently the overestimation of Δn_{app} and subsequently τ_{app} decreases (Figure 3, Table II).

B. Variation of the RAT-state density N_{RAT}

With an increasing concentration of RAT-defects N_{RAT} (and $\sigma_{n,RAT} > 0$), the recombination lifetime τ_r in low level injection decreases according to the SRH-formalism. At the same time, a higher maximum value of minority charge carriers can be captured in the RAT-defects and so the difference between Δp and Δn becomes larger. That leads to an increased Δn_{app} and hence to an increased apparent lifetime τ_{app}.

As known from the H&H case $\Delta n = N_{RAT}$ denotes the excess charge carrier concentration where the trapping effects begin to obscure the recombination lifetime by an increased apparent lifetime (Figure 4, Table III).

C. Variation of the RAT-state energy level E_{RAT}

Using SRH statistics to describe the decreased low level injection lifetime due to the presence of RAT states shows yet another difference to the H&H model: The exaggerated apparent lifetime towards low carrier injection saturates at a certain lifetime value, which depends on the energy level of the trap state. This saturated apparent lifetime towards $\Delta n < N_{RAT}$ could therefore be used for the determination of the energy level of the trap state. However, as illustrated in Figure 5, the saturation value of the apparent carrier lifetime at $\Delta n \ll N_{RAT}$ not only depends on the energy level E_{RAT} of the RAT-defect but also on the majority capture cross section $\sigma_{p,RAT}$ (Figure 5, Table IV). Thus, determining the energy level E_{RAT} by the H&H model[26] is likely to produce erroneous results if interaction between trap and majority carriers cannot be excluded.

In the H&H case (dashed lines), i.e., $\sigma_{p,RAT} = 0$, the apparent lifetime increases the closer the trap-level lies to the valence band. An exception are traps lying very close to the valence band; such H&H traps lower than the Fermi level are almost completely filled even in the dark and therefore do not cause much trapping under illumination. However, the use of RAT-state properties reveals (as opposed to the prediction of the H&H model) that the apparent lifetime decreases for RAT-states lying close to the valence band (case C in Figure 5): In this situation, the RAT-defect loses its trap-character because the recombination-path from the

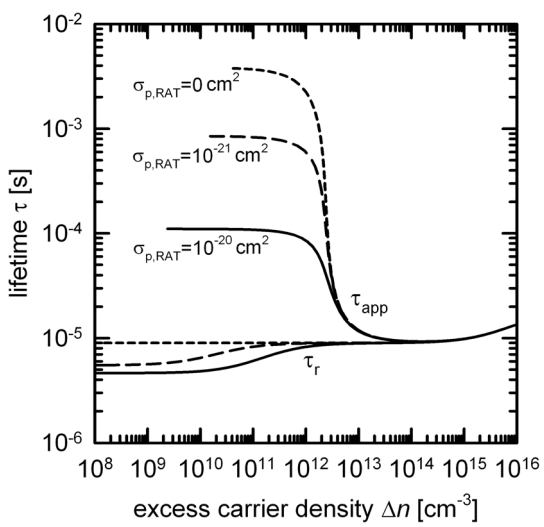

FIG. 3. Apparent lifetime τ_{app} and recombination lifetime τ_r for variations of the majority capture cross section of the RAT-defect.

TABLE II. Defect parameters related to Figure 3.

Parameter	SRH-state	RAT-state
E_t - E_V (eV)	0.55	0.55
N_t (cm^{-3})	1×10^{13}	1×10^{13}
σ_n (cm^2)	1×10^{-15}	1×10^{-15}
σ_p (cm^2)	1×10^{-15}	Variable

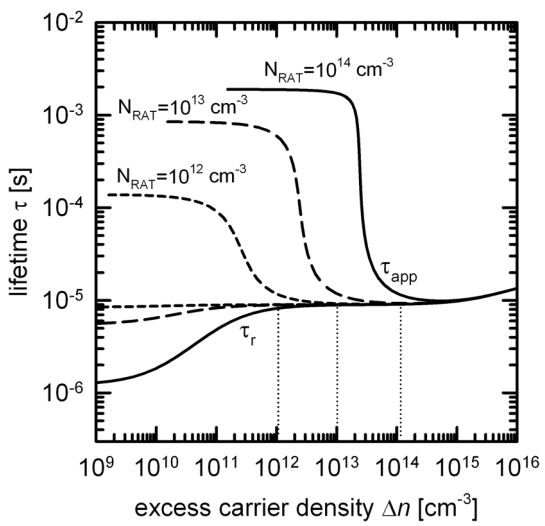

FIG. 4. Apparent lifetime τ_{app} and total recombination lifetime τ_r for variations of the RAT density N_{RAT}. With increasing N_{RAT} the apparent lifetime increases and the recombination lifetime decreases.

TABLE III. Defect parameters related to Figure 4.

Parameter	SRH-state	RAT-state
E_t - E_V (eV)	0.55	0.55
N_t (cm^{-3})	1×10^{13}	Variable
σ_n (cm^2)	1×10^{-15}	1×10^{-15}
σ_p (cm^2)	1×10^{-15}	1×10^{-21}

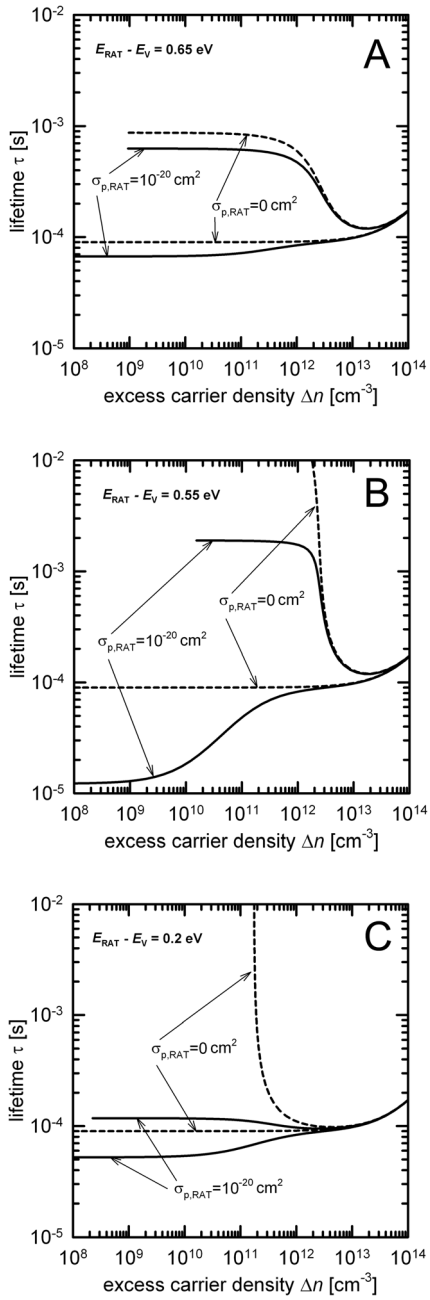

FIG. 5. Apparent lifetime τ_{app} and recombination lifetime τ_r for variations of the RAT energy level E_{RAT} for $\sigma_{p,RAT} = 10^{-20}\,cm^2$ (solid lines) and $\sigma_{p,RAT} = 0\,cm^2$ (dashed lines).

RAT-state to the valence band now opens up and electrons are not only trapped but recombine with the majority carriers according to the SRH formalism. The associated transition rate is: $R_{RAT\rightarrow VB} = f_{RAT} \cdot N_{RAT} \cdot \sigma_{p,RAT} \cdot v_{th} \cdot p$, where f_{RAT} is the occupation probability of the RAT-state and v_{th} is the thermal velocity. For RAT-energy-levels close to the valence band f_{RAT} has a large value and therefore the rate of electrons passing to the valence band is high in this case.

In the H&H model (dashed lines), i.e., $\sigma_{p,RAT} = 0$, the trapping centers do not affect the recombination lifetime. In contrast to that the recombination lifetime behavior in our model, i.e.$\sigma_{p,RAT} > 0$, depends on the energy level of the RAT-state. Like the SRH-formalism predicts, the lifetimes for defects close to the middle of the bandgap (case B) are smaller than for defects close to the energy bands (cases A and C).

TABLE IV. Defect parameters related to Figure 5.

Parameter	SRH-state	RAT-state
E_t - E_V (eV)	0.55	Variable
N_t (cm^{-3})	1×10^{12}	1×10^{13}
σ_n (cm^2)	1×10^{-15}	1×10^{-16}
σ_p (cm^2)	1×10^{-15}	1×10^{-20}/zero

III. EXPERIMENTAL RESULTS

To provide experimental proof of our predictions, we perform the following experiment: We use adjacent wafers of the same p-type multicrystalline (mc) silicon ingot with a resistivity of 1.7 Ωcm and a thickness of 200 μm. Therefore, we can expect the same lateral structures and material properties for the wafers. All wafers were phosphorus gettered at 900 °C. Half of the samples were then deposited with remote PECVD SiN_x with a refractive index of $n = 2.05$ and a thickness of 80 nm in an Oxford Plasmalab 80 Plus and after that fired in a belt furnace at 900 °C. This process leads to a passivation of the wafer volume: at high temperatures elemental hydrogen can diffuse into the wafer volume and saturate defect states within the bandgap which are causal for recombination and trapping effects.[27] After the firing step the SiN_x and the phosphorus emitter of all samples were etched away. To allow bulk lifetime measurements, the surface of all samples were passivated with 80 nm SiN_x. When applied to single-crystalline floating-zone (FZ) silicon, this SiN_x passivation scheme is sufficient to produce effective carrier lifetimes well beyond 1000 μs, which is about an order of magnitude larger than any effective carrier lifetime measured on the mc wafers of our investigation. Hence, we are able to interpret the effective lifetime data as measured on the mc-Si samples as a good approximation to the carrier lifetime in the bulk.

In Figure 6, we present lifetime measurements of one of the fired sample (circles) and one of the not-fired sample (triangles). We accomplished QSSPC-[14] (open symbols) and PL-[25] (filled symbols) lifetime measurements at the same position on the wafers to assure comparability between the measurements. The measurement setup can be seen in Ref. 25.

In regions of low level injection, the QSSPC method is prone to trapping induced effects which results in an overestimated lifetime. In the following, we therefore call the lifetime determined with the QSSPC method apparent lifetime τ_{app}. In contrast to that the PL method is not prone to trapping effects and therefore the PL lifetime can be identified with the recombination lifetime τ_r.

The overestimation of the apparent lifetime of the fired sample (circles) occurs at $\Delta n < 4 \times 10^{13}\,cm^{-3}$, and for the not-fired sample (triangles) at $\Delta n < 1 \times 10^{14}\,cm^{-3}$. From the injection density where the symptomatic rise of the apparent lifetime occurs, we can conclude that there are more trap-like defects in the not-fired sample than in the fired sample.[28] Additionally, the fired sample shows a higher recombination

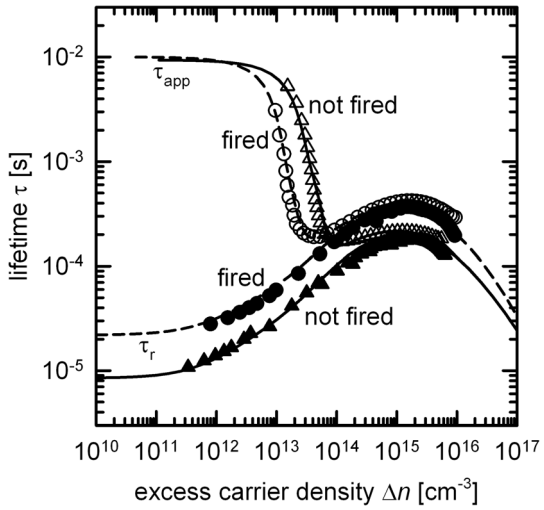

FIG. 6. Lifetime data of mc-Si samples with (circles) and without (triangles) firing step from QSSPC- (open symbols) and photoluminescence-(filled symbols) measurements and fit (lines) of the lifetime data using SRH statistics and the defect parameters presented in Table V.

lifetime in low level injection than the not-fired sample. Due to the same SiN_x passivation of both samples, we can assume that the SiN_x passivation of the surfaces is not causal for the different lifetime characteristics of both samples.

In Figure 6, we fitted the measured data using our model (lines). To fit the data in the trapping-free region, two SRH defects were necessary. The need for a second recombination active state near to the conduction band to fit experimental lifetime data was reported before.[29] To simulate the trapping behavior, we additionally assume two RAT defects in the bandgap. Note that we examine a mc sample in this experiment that is likely to harbor a comparatively high number of different types of crystal defects and impurities. Therefore, it appears justified to take into account a second type of RAT defect to describe the measured data. The parameters of the SRH defects and of the RAT defects are given in Table V.

It is observable that the defect parameters to fit the measured lifetime data are the same for both samples except the defect concentrations. That complies with the physical reality that both wafers are of the same material. It can be interpreted that the hydrogen passivation of the wafer volume of the fired sample does not change the recombination relevant defects but fractionally saturates them. The concentrations of all defect states of the not-fired sample are about twice as high as the defect concentrations of the fired sample. That suggests that all participating defects are related to one sort of defect (crystal defect or impurity) and so are saturated with the same probability and portion by the hydrogen. Additionally, the experimental lifetime data show that the recombination lifetime tends towards saturation in low level injection. That is in good agreement with the prediction of the model.

A rise of the apparent lifetime at higher injection densities can be interpreted as a warning in terms of a reduced recombination lifetime. Both samples have the same lifetime value $\tau_{app} = 180\,\mu s$ at the injection level where trapping effects begin to masked the recombination lifetime in low level injection at QSSPC measurements. But the recombination lifetime for low injection densities is much lower for the "not-fired" sample, which inhibits more trapping related defects than for the fired sample.

For this reason, we compare lifetime measurements of two comparable standard solar cells: i.e., both cells are fabricated on wafers of the same column of the same mc silicon ingot. This is the same material as used in our aforementioned experiments with a resistivity of 1.7 Ω cm. One of the cells passed through a "firing step" during its fabrication (circles), whereas the other cell did not see a "firing step" (triangles).

We measured the J_{SC}-V_{OC} curves of the cells that are shown in Figure 7(a). Therewith we calculated the recombination lifetime[30,31] for the range of higher voltages as indicated in Figure 7, where the J_{SC}-V_{OC} curves are not affected by shunts. The obtained data are shown in Figure 7(b) as filled symbols. Note that this calculated recombination lifetime from the J_{SC}-V_{OC} curves of our solar cells gives the same information as PL measurements on lifetime samples.

To allow QSSPC lifetime measurements, we etched away the metal from both sides of the cells with boiling HCl. In the following, we assume that the effective surface recombination velocity (SRV) of the metalized cells does not noticeable differ from the SRV of the not-metalized cells, i.e., we interpret the effective carrier lifetimes calculated from the J_{SC}-V_{OC} curves as a reasonable approximation to the bulk lifetime as measured by the etched-off lifetime samples that are passivated with SiN. Note that this assumption is well satisfied as the open-circuit voltages of these cells are far below those values that are achievable with the present emitters and surface passivations. Therefore, the cells are dominated by the bulk recombination and the J_{SC}-V_{OC} data are a good indication of the bulk lifetime. After etching off the metals, we performed QSSPC measurements of the carrier lifetimes. The results are also shown in Figure 7(b) as open symbols.

Both cells show an increase of the apparent carrier lifetime towards low injection levels in the QSSPC measurements. However, the "fired" cell shows its trapping-induced increase of the apparent lifetime at excess carrier densities of

TABLE V. Defect parameters related to Figure 6.

Parameter	1. SRH-state	2. SRH-state	1. RAT-state	2. RAT-state
N_t ("not-fired") (cm^{-3})	6.0×10^{11}	1.0×10^{11}	1.2×10^{14}	1.0×10^{14}
N_t ("fired") (cm^{-3})	3.0×10^{11}	6.0×10^{10}	4.0×10^{13}	5.0×10^{13}
E_t - E_V (eV)	0.55	1.00	0.55	0.58
σ_n (cm^2)	5×10^{-15}	1×10^{-13}	6×10^{-17}	1×10^{-15}
σ_p (cm^2)	1×10^{-17}	1×10^{-13}	7×10^{-21}	$\leq 1 \times 10^{-23}$

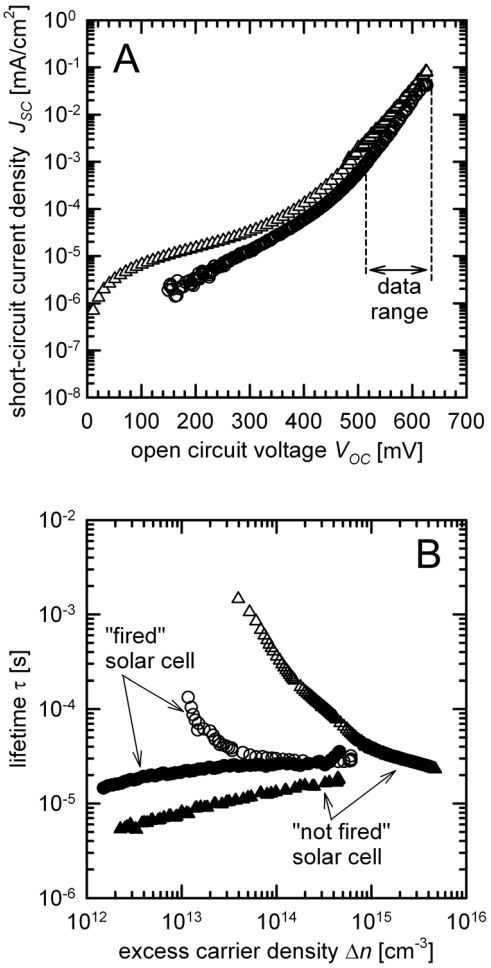

FIG. 7. (a) J_{SC}-V_{OC} curves of two solar cells. The marked data range shows the data points that are used to calculate the recombination lifetime. (b) Calculated recombination lifetime (filled symbols) and QSSPC measurements (open symbols) of the cells.

about two orders of magnitude lower than the "not-fired" cell. Concurrently, the recombination lifetime of the "fired" sample is higher than that of the "not-fired" sample. That seems to strengthen our predicted correlation between the existence of trapping inducing defects and a reduced recombination lifetime in low level injection.

IV. CONCLUSION

We have shown that the observation of both, the diverging increased apparent lifetime (photo conductance measurements) and the decreasing recombination lifetime (photoluminescence measurements) can be explained by a single physical mechanism; i.e., by RAT states. These RAT defects have cross sections for capturing majority charge carriers larger than zero, but potentially several orders of magnitude smaller than for capturing minority carriers. This asymmetry gives rise to trapping effects that obscures the recombination lifetime by an increased apparent lifetime in, e.g., photoconductivity based lifetime measurements. However, the RAT states additionally decrease the recombination lifetime in low level injection as it can be observed by photoluminescence based lifetime measurements or by the performance of solar cells. Such conclusion agrees well with the observation that regions of high trapping activity in mc-Si wafers turn out to be badly performing regions of final processed solar cells.[32] Trapping should therefore be considered as an indication for hidden, yet potentially strongly increased, low injection recombination activity.

[1]W. Shockley and W. T. Read, "Statistics of the recombinations of holes and electrons," Phys. Rev. **87**, 835 (1952).
[2]R. N. Hall, "Electron-hole recombination in germanium," Phys. Rev. **87**, 387 (1952).
[3]W. van Roosbroeck and W. Shockley, "Photon-radiative recombination of electrons and holes in germanium," Phys. Rev. **94**, 1558 (1954).
[4]T. Trupke, M. A. Green, P. Würfel, P. P. Altermatt, A. Wang, J. Zhao, and R. Corkish, "Temperature dependence of the radiative recombination coefficient of intrinsic crystalline silicon," J. Appl. Phys. **94**, 4930 (2003).
[5]W. P. Dumke, "Spontaneous radiative recombination in semiconductors," Phys. Rev. **105**, 139 (1957).
[6]M. S. Tyagi and R. van Overstraeten, "Minority carrier recombination in heavily doped silicon," Solid State Electron. **26**, 577 (1983).
[7]D. B. Laks and G. F. Neumark, "Accurate interband-Auger-recombination rates in silicon," Phys. Rev. B **42**, 5176 (1990).
[8]P. T. Landberg, "Trap-Auger recombination in silicon of low carrier densities," Appl. Phys. Lett. **50**, 745 (1987).
[9]A. Hangleiter and R. Häcker, "Enhancement of band-to-band auger recombination by electron-hole correlations," Phys. Rev. Lett. **65**, 215 (1990).
[10]P. P. Altermatt, J. Schmidt, G. Heiser, and A. G. Aberle, "Assessment and parameterisation of Coulomb-enhanced Auger recombination coefficients in lowly injected crystalline silicon," J. Appl. Phys. **82**, 4938 (1997).
[11]A. Richter, F. Werner, A. Cuevas, J. Schmidt, and S. W. Glunz, "Improved parameterization of Auger recombination in silicon," Energy Procedia **27**, 88–94 (2012).
[12]Y. C. Cheng, "Electronic states at the silicon-silicon interface," Prog. Surf. Sci. **8**, 181 (1977).
[13]A. G. Aberle, S. Glunz, and W. Warta, "Impact of illumination level and oxide parameters on Shockley-Read-Hall. recombination at the Si-Si02 interface," J. Appl. Phys. **71**, 4422 (1992).
[14]R. A. Sinton and A. Cuevas, "Contactless determination of current–voltage characteristics and minority carrier lifetimes in semiconductors from quasi-steady-state photoconductance data," Appl. Phys. Lett. **69**, 2510 (1996).
[15]M. Bail, J. Kentsch, R. Brendel, and M. Schulz, "Lifetime mapping of silicon wafers by an infrared camera," in *Proceedings of the 28th IEEE PVSC*, Anchorage, USA, 2000, pp. 100–103.
[16]S. Riepe, J. Isenberg, C. Ballif, S. W. Glunz, and W. Warta, "Carrier density and lifetime imaging of silicon wafers by infrared lock-in thermography," in *Proceedings of the 17th EU-PVSEC*, Munich, Germany, 2001, pp. 1597–1599.
[17]J. R. Haynes and J. A. Hornbeck, "Temporary traps in silicon and germanium," Phys. Rev. **90**, 152 (1953).
[18]J. A. Hornbeck and J. R. Haynes, "Trapping of minority carriers in silicon: I. p-type silicon," Phys. Rev. **97**, 311 (1955).
[19]J. R. Haynes and J. A. Hornbeck, "Trapping of minority carriers in silicon: II. n-type silicon," Phys. Rev. **100**, 606 (1955).
[20]K. R. McIntosh, B. B. Paudyal, and D. H. Macdonald, "Generalized procedure to determine the dependence of steady-state photoconductance lifetime on the occupation of multiple defects," J. Appl. Phys. **104**, 084503 (2008).
[21]N. P. Harder, R. Gogolin, and R. Brendel, "Trapping-related recombination of charge carriers in silicon," Appl. Phys. Lett. **97**, 112111 (2010).
[22]D. Macdonald and A. Cuevas, "Trapping of minority carriers in multicrystalline silicon," Appl. Phys. Lett. **74**, 1710 (1999).
[23]T. Trupke, R. A. Bardos, M. C. Schubert, and W. Warta, "Photoluminescence imaging of silicon wafers," Appl. Phys. Lett. **89**, 044107 (2006).
[24]R. A. Bardos, T. Trupke, M. C. Schubert, and T. Roth, "Trapping artifacts in quasi-steady-state photoluminescence and photoconductance lifetime measurements on silicon wafers," Appl. Phys. Lett. **88**, 053504 (2006).
[25]S. Herlufsen, J. Schmidt, D. Hinken, K. Bothe, and R. Brendel, "Photoconductance-calibrated photoluminescence lifetime imaging of crystalline silicon," Phys. Status Solidi (RRL) **2**, 245 (2008).
[26]J. Schmidt, K. Bothe, and R. Heezel, "Oxygen-related minority-carrier trapping centers in p-type Czochalski silicon," Appl. Phys. Lett. **80**, 4395 (2002).

[27]C. Ulzhoefer, B. Wolpensinger, and J. Schmidt, "Understanding the lifetime evolution in n-type multicrystalline silicon during phosphorus gettering and hydrogenation," EPVSEC (2008).
[28]D. MacDonald and A. Cuevas, "Understanding carrier trapping in multicrystaline silicon," Sol. Energy Mater. Sol. Cells **65**, 509–516 (2001).
[29]J. Schmidt and A. Cuevas, "Electronic properties of light-induced recombination centers in boron-doped Czochralski silicon," J. Appl. Phys. **86**, 3175 (1999).
[30]R. A. Sinton and A. Cuevas, "A quasi-steady-state open-circuit voltage method for solar cell characterization," 16th European Photovoltaik Solar Energy Conference (Glasgow, UK, May 2000).
[31]M. Kerr, A. Cuevas, and R. A. Sinton, "Generalized analysis of quasi-steady-state and transient decay open circuit volage measurements," J. Appl. Phys. **91**, 399 (2002).
[32]M Schubert and W. Warta, "Prediction of diffusion length in multicrystalline silicon solar cells from trapping images on starting material," Prog. Photovoltaics **15**(4), 331–336 (2007).